Simultaneous heat and mass transfer in laminar mixed convection flows between vertical parallel plates with asymmetric heating

W. M. Yan, Y. L. Tsay, and T. F. Lin
Department of Mechanical Engineering, National Chiao Tung University, Hsinchu, Taiwan, Republic of China

This study investigated the role of vaporization or condensation of the water vapor on the wetted channel walls in laminar mixed convection flows under the simultaneous influences of combined buoyancy effects of thermal and mass diffusion. Major nondimensional groups identified are Gr_T, Gr_M, Re, Pr, and Sc. Results are specifically presented for an air–water system under various heating conditions. The effects of the wetted wall temperatures and the Reynolds number on the momentum, heat and mass transfer are examined in great detail. Results show that the effects of the evaporation or condensation of the water vapor along the wetted walls on the laminar mixed convection heat transfer are rather substantial.

Keywords: heat and mass transfer; mixed convection; latent heat transfer; asymmetric heating

Introduction

Transport processes in which the combined buoyancy forces of heat and mass transfer, resulting from the simultaneous presence of differences in temperature and variations in concentration, have significant influences on momentum, heat and mass transfer in flowing gas mixtures are often encountered in many engineering systems and the natural environment. Windy-day evaporation and vaporization of moist and fog, distillation of a volatile component from a mixture with involatiles, the process of evaporative cooling for waste heat disposal, and cooling of a high temperature surface by coating it with phase-change material are just some prominent examples of such processes in which mass transfer operations are accompanied by the transfer of heat.

The effects of mass diffusion on natural convection heat transfer have been widely studied for external flow systems[1–4] and internal flow systems.[5,6] Concerning forced convection flows, combined heat and mass transfer in laminar flows were examined by Chow and Chung[7] and Wu *et al.*[8] While for mixed convection, Santarelli and Foraboschi[9] investigated the effects of natural convection on reaction and heat transfer parameters for a laminar fluid flow undergoing a chemical reaction. Recently, Yeh *et al.*[10] numerically examined the effect of heat and mass transfer on laminar mixed convection heat transfer over a horizontal plane.

Despite its importance in engineering applications, the combined buoyancy effects of thermal and mass diffusion on forced convection channel flows have not received much attention. Recognizing the relatively little research on the internal mixed convection flow, the present authors[11] performed an analysis of combined buoyancy effects of thermal and mass diffusion on laminar forced convection heat transfer in a vertical tube, particularly for an air–water vapor mixture.

Address reprint requests to Dr. Yan at the Department of Mechanical Engineering, National Chiao Tung University, Hsinchu, Taiwan 30049, Republic of China.

Received 18 February 1988; accepted 26 January 1989

In the present study, the geometry to be examined is a mixed convection flow in a pair of long vertical parallel plates with channel width b. Both of the channel walls are wetted by thin liquid water films. The right and left walls are kept at uniform but different temperature levels, T_1 and T_2, respectively, higher than the ambient temperature T_0. The flow of moist air, initially stationary, in the channel is initiated by a mechanical device as well as by the combined buoyancy forces due to differences in temperature and in concentration of water vapor between the liquid films and the ambient. Attention is focused on the study of the effects of the coupled thermal and mass diffusion on the steady developments of the velocity, temperature and concentration fields in the flows of a dry air–water vapor mixture. Particular attention is paid to the investigation of the latent heat transport in conjunction with the evaporation or condensation of the water vapor along the wetted walls.

Analysis

In an initial effort to study the mass diffusion effects in mixed convection flows, the liquid films on the wetted walls are assumed to be extremely thin so that they can be regarded as the boundary conditions for heat and mass transfer. Both films are stationary and at the same uniform temperatures with the channel walls T_1 and T_2, respectively. In reality the liquid films are finite in thickness. Hence the films could move upwards or downwards, and the shapes of the liquid–gas interfaces could be quite complex. As a result, the momentum, heat and mass transfer in both the films should also be analyzed with the interfacial phenomena appropriately treated. This would, however, greatly complicate the analysis and make the theoretical work formidable. The influences of the finite liquid films on the heat transfer may not be properly assessed without the help from the experimental study which will be conducted shortly. The results from the present analysis are therefore only valid for the limiting condition of extremely thin liquid films.

By introducing the Boussinesq approximation (the concentration of water vapor in the mixture being very low and the

temperature nonuniformity in the system being small), the steady laminar mixed convection flow of moist air in a vertical channel resulting from the combined buoyancy effects of thermal and mass diffusion can be described by the basic equations, in dimensionless form, as:

continuity equation

$$\frac{\partial U}{\partial X}+\frac{\partial V}{\partial Y}=0 \tag{1}$$

axial-momentum equation

$$U\frac{\partial U}{\partial X}+V\frac{\partial U}{\partial Y}=-\frac{\mathrm{d}P}{\mathrm{d}X}+\frac{\partial^2 U}{\partial Y^2}+\frac{2(\mathrm{Gr}_T\cdot\theta+\mathrm{Gr}_M\cdot W)}{\mathrm{Re}} \tag{2}$$

energy equation

$$U\frac{\partial \theta}{\partial X}+V\frac{\partial \theta}{\partial Y}=\frac{1}{\mathrm{Pr}}\frac{\partial^2\theta}{\partial Y^2}+\frac{A}{\mathrm{Sc}}\cdot\frac{\partial\theta}{\partial Y}\cdot\frac{\partial W}{\partial Y} \tag{3}$$

equation of species diffusion for water vapor

$$U\frac{\partial W}{\partial X}+V\frac{\partial W}{\partial Y}=\frac{1}{\mathrm{Sc}}\cdot\frac{\partial^2 W}{\partial Y^2} \tag{4}$$

Here the dimensionless quantities are defined in the following:

$$X=\frac{2x}{b\cdot\mathrm{Re}} \qquad Y=\frac{y}{b}$$

$$U=\frac{u}{u_0} \qquad V=\frac{vb}{\nu}$$

$$\theta=\frac{T-T_0}{T_1-T_0} \qquad W=\frac{w-w_0}{w_r-w_0}$$

$$P=\frac{p-p_0}{\rho u_0^2} \qquad \mathrm{Re}=\frac{u_0\cdot 2b}{\nu} \tag{5}$$

$$\mathrm{Gr}_T=\frac{g(T_1-T_0)b^3}{T_0\nu^2} \qquad \mathrm{Gr}_M=\frac{g(M_a/M_v-1)(w_r-w_0)b^3}{\nu^2}$$

$$r_T=\frac{T_2-T_0}{T_1-T_0}$$

Here w_r is the saturated mass fraction of water vapor at T_1 and $p_o\cdot\mathrm{Gr}_T$ and Gr_M are respectively the Grashof numbers for heat and mass transfer. It should be noted that the last term on the right side of Equation 3 represents the energy transport through the interdiffusion of the species, air and water vapor. The third term on the RHS of Equation 2 is the buoyancy term.

By using the equation of state for an ideal gas mixture and assuming a low level of water vapor concentration in the flow, the density variation in the moist air can be approximated by

$$\frac{\rho_0-\rho}{\rho}=\frac{T-T_0}{T_0}+\left(\frac{M_a}{M_v}-1\right)(w-w_0) \tag{6}$$

Moreover, by assuming the moist air–liquid film interfaces to be in thermodynamic equilibrium, the interfacial mass fraction of water vapor on both of the wetted walls can be evaluated

Notation

A	$[(C_{pv}-C_{pa})/C_p](w_r-w_0)$
b	Channel width
C_p	Specific heat
D	Mass diffusivity
g	Gravitational acceleration
Gr_M	Grashof number (mass transfer)
Gr_T	Grashof number (heat transfer)
h_{fg}	Latent heat of vaporization
h_M	Local mass transfer coefficient
k	Thermal conductivity
M	Molecular weight
M_r	Nondimensional film evaporation rate
Nu_l	Local Nusselt number (latent heat or enthalpy transfer)
Nu_s	Local Nusselt number (sensible heat or heat transfer)
Nu_x	Overall local Nusselt number
p	Pressure of the moist air in the channel
P	Dimensionless motion pressure (pressure defect)
p_m	Motion pressure (pressure defect)
p_0	Ambient pressure
Pr	Prandtl number, ν/α
p_1, p_2	Partial pressure of water vapor at wetted walls 1 and 2, respectively
Q	Total heat transfer rate
Q''	Total heat transfer rate without liquid water film
q''	Interfacial energy flux flowing into air stream
Re	Reynolds number at the inlet, $u_0(2b)/\nu$
r_T	Temperature ratio
S	Parameter, Equation 15
Sc	Schmidt number, ν/D
Sh	Local Sherwood number
T	Temperature
u	Axial velocity
u_0	Average inlet velocity
U	Dimensionless axial velocity
v	Transverse velocity
V	Dimensionless transverse velocity
V_r	Dimensionless velocity ratio, v/u_0
w	Mass fraction of water vapor
W	Dimensionless mass fraction of water vapor
w_r	Saturated mass fraction of water vapor at T_1 and p_0
w_1, w_2	Saturated mass fraction of water vapor on the right and left wetted walls, respectively
x	Axial coordinate
X	Dimensionless axial coordinate
y	Transverse coordinate
Y	Dimensionless transverse coordinate
α	Thermal diffusivity
θ	Dimensionless temperature
ν	Kinematic viscosity
ρ	Density
ϕ	Relative humidity of air at ambient condition

Subscripts

a	Of air
b	Bulk quantity
0	At inlet condition
r	At reference condition
v	Of water vapor
1	Condition at right wetted wall (i.e., at $y=b$)
2	Condition at left wetted wall (i.e., at $y=0$)

by the equation

$$w_i = \frac{p_i M_v}{p_i M_v + (p - p_i) M_a} \qquad i = 1, 2 \tag{7}$$

where p_1 (p_2) is the partial pressure of water vapor on the right (left) wetted wall. It should be mentioned here that w_1 and w_2 depend on the mixture pressure p, and thus they vary with x. This prevents us from taking either of w_1 or w_2 as a reference value in the nondimensionalization process. Instead w_r is employed. In the present study, the thermophysical properties of the mixture are taken to be constant and are evaluated by the one-third rule. This special way of computing the properties is found to be appropriate for the study of combined heat and mass transfer problems.[7,12] The complete details on the evaluation of properties of air, water vapor and their mixture are available in Refs. 11 and 13.

The governing equations are subjected to the following boundary conditions:

$$\begin{aligned} &X=0 \quad U=1 \quad \theta=0 \quad W=0 \quad P=0 \\ &Y=0 \quad U=0 \quad V=V_2 \quad \theta=r_T \quad W=\frac{w_2-w_0}{w_r-w_0} \\ &Y=1 \quad U=0 \quad V=V_1 \quad \theta=1 \quad W=\frac{w_1-w_0}{w_r-w_0} \end{aligned} \tag{8}$$

Notice that the air–water interfaces are semipermeable, that is, the solubility of air in water is negligibly small and air is stationary at the interfaces, the transverse velocity of the mixture on both of the wetted walls can be evaluated by

$$V_i = -\frac{w_r - w_0}{1 - w_i} \cdot \frac{1}{\mathrm{Sc}} \cdot \left.\frac{\partial W}{\partial Y}\right|_i \qquad i = 1, 2 \tag{9}$$

One constraint to be satisfied in the solution of a steady channel flow is the overall mass balance at every axial location.

$$\int_0^1 U \, \mathrm{d}y = 1 - \int_0^X V_1 \, \mathrm{d}X + \int_0^X V_2 \, \mathrm{d}X \tag{10}$$

The above equation is used in the solution process to determine the pressure gradient in the flow.

Energy transport between the wetted walls and the moist air in the presence of mass transfer depends on two related factors: the fluid temperature gradient at the channel wall, resulting in a sensible heat transfer, and the rate of mass transfer, resulting in a latent heat transfer.[14,15] The total energy fluxes from the wetted walls are given by

$$q_1'' = q_{s1}'' + q_{l1}'' = k \left.\frac{\partial T}{\partial y}\right|_{y=b} + \frac{\rho \mathrm{Dh}_{fg1}}{1 - w_1} \cdot \left.\frac{\partial w}{\partial y}\right|_{y=b} \tag{11a}$$

$$q_2'' = q_{s2}'' + q_{l2}'' = -k \left.\frac{\partial T}{\partial y}\right|_{y=0} - \frac{\rho \mathrm{Dh}_{fg2}}{1 - w_2} \cdot \left.\frac{\partial w}{\partial y}\right|_{y=0} \tag{11b}$$

Notice that sensible heat transfer and latent heat transfer are frequently referred to heat flux and enthalpy flux, respectively. The local Nusselt numbers are defined as

$$\mathrm{Nu}_{xi} = \frac{h_i b}{k} = \frac{q_i''}{k(T_1 - T_b)/b} \qquad i = 1, 2 \tag{12}$$

which can be written as

$$\mathrm{Nu}_{xi} = \mathrm{Nu}_{si} + \mathrm{Nu}_{li} \qquad i = 1, 2 \tag{13}$$

where

$$\mathrm{Nu}_{s1} = \frac{1}{1 - \theta_b} \cdot \left.\frac{\partial \theta}{\partial Y}\right|_{Y=1} \qquad \mathrm{Nu}_{s2} = \frac{-1}{1 - \theta_b} \cdot \left.\frac{\partial \theta}{\partial Y}\right|_{Y=0} \tag{14a}$$

$$\mathrm{Nu}_{l1} = \frac{S_1}{(1 - w_1)(1 - \theta_b)} \cdot \left.\frac{\partial W}{\partial Y}\right|_{Y=1}$$

$$\mathrm{Nu}_{l2} = \frac{-S_2}{(1 - w_2)(1 - \theta_b)} \cdot \left.\frac{\partial W}{\partial Y}\right|_{Y=0} \tag{14b}$$

Here S_1 and S_2 signify the relative importance of energy transport through species diffusion to that through thermal diffusion on the right and left wetted walls, respectively,

$$S_i = \frac{\rho \mathrm{Dh}_{fgi}(w_r - w_0)}{k(T_1 - T_0)} \qquad i = 1, 2 \tag{15}$$

Similarly, the local Sherwood numbers at the air–water interfaces are

$$\mathrm{Sh}_1 = \frac{h_{M1} b}{\mathrm{D}} = \frac{(w_r - w_0)}{(w_1 - w_b)} \cdot \left.\frac{\partial W}{\partial Y}\right|_{Y=1} \tag{16a}$$

$$\mathrm{Sh}_2 = \frac{h_{M2} b}{\mathrm{D}} = \frac{-(w_r - w_0)}{(w_1 - w_b)} \cdot \left.\frac{\partial W}{\partial Y}\right|_{Y=0} \tag{16b}$$

Solution method

Because the flow under consideration is a boundary layer type, the solution for Equations 1–4 can be marched in the downstream direction. A fully implicit numerical scheme in which the axial convection is approximated by the upstream difference and transverse convection and diffusion terms by the central difference is employed to transform the governing equations into finite-difference equations. Each system of the finite-difference equations forms a tridiagonal matrix equation which can be efficiently solved by the Thomas algorithm.[16] The detailed solution procedures are similar to those in Ref. 11.

To obtain enhanced accuracy in the numerical computations, grids are chosen to be uniform in the y direction but nonuniform in the x direction to account for the drastic variations of velocity, temperature, and concentration in the near-entrance region. Several arrangements of grid points in x and y directions are tested and the corresponding results are presented in Table 1. It is found from the table that the differences in the local Nusselt number for the computations by using 101×81 and 201×161 grids are always less than 2%. Accordingly, the computation for the 101×81 grid is sufficient for the understanding of the heat and mass transfer characteristics in the flow. The results to be presented are computed by using 101×81 grid.

To further check the adequacy of the numerical scheme used in the present study, the results for the limiting case of laminar forced convection flows in the channel influenced by the buoyancy force of thermal diffusion alone were first obtained.

Table 1 Comparison of local Nusselt numbers Nu_{x1} for various grid arrangements for case II

X	201×161	201×81	101×161	101×81	51×81	51×41
0.00076	81.05	78.06	81.56	82.14	79.75	76.97
0.0067	39.31	39.42	39.23	38.92	37.41	37.18
0.0595	22.63	22.60	22.51	22.70	22.82	22.71
0.56	17.97	17.97	17.97	17.97	17.97	17.98

Excellent agreement between the present predictions and those of Aung and Worku[17,18] was found.

Results and discussion

In the present study, calculations are specifically performed for moist air flowing in the channel, a situation widely found in engineering systems. Other mixtures can be solved in the same way. It should be emphasized that not all the nondimensional groups appearing in the study, i.e., Pr, Sc, Re, Gr_T, etc., can be arbitrarily assigned. In fact, they are interdependent for a given mixture under certain specific conditions. In light of practical situations, T_0, T_1, T_2, ϕ, and Re are selected as the independent parameters. The following conditions are selected in the computations: Unsaturated moist air with a relative humidity of 50% at 20°C and 1 atm enters the long vertical parallel plates with channel width 1.5 cm from the bottom end by the combined action of a certain external force as well as the buoyancy forces of heat and mass diffusion. All the nondimensional parameters can then be evaluated except the inlet Reynolds number, which should be specified separately. The results are obtained for several cases presented in Table 2.

Figure 1 illustrates the developments of the dimensionless axial velocity profiles. For comparison purpose, the results without mass diffusion effect are presented in Figures 1(c) and 1(d). It is clearly seen in these plots that the velocity profiles develop gradually from the uniform distributions at the inlet to the distorted ones in the downstream region with the maximum velocity near the hotter wall (right wall). This is due to larger buoyancy forces near the right wetted wall. Moreover, the peak in the velocity profile grows as the moist air moves further downstream. Also noted is the larger flow acceleration for the case with the lower Re. Comparing Figures 1(a) with 1(c) or Figures 1(b) with 1(d) indicates that the magnitude of the velocity component U is larger for the cases with mass diffusion buoyancy effect relative to those without mass transfer.

The developments of dimensionless temperature and mass-fraction are shown in Figures 2 and 3, respectively. It is interesting to observe that both θ and W develop in a very similar fashion. Careful inspection, however, discloses that the concentration boundary layers develop a little more rapidly than the thermal boundary layers. This simply results from the fact that Pr is slightly larger than Sc in the flow. Also seen in Figure 3 is that in the initial portion of the channel, the mass-fraction of water vapor in the flow is still small relative to those on both the wetted walls. But as the moist air goes downstream, the mass-fraction of the water vapor in the flow increases and the concentration level of water vapor near the left wetted wall could be over w_2 at certain axial location. This is clearly seen in Figure 3 for the curve for $X=0.49$. Condensation of water vapor contained in the moist air on the left wetted wall thus occurs in this downstream region. One point worth mentioning is that because of the small pressure defect in the flow as evident in Figure 4, w_1 is almost equal to w_v, and hence W_1 is very close to 1. In the separate computation,

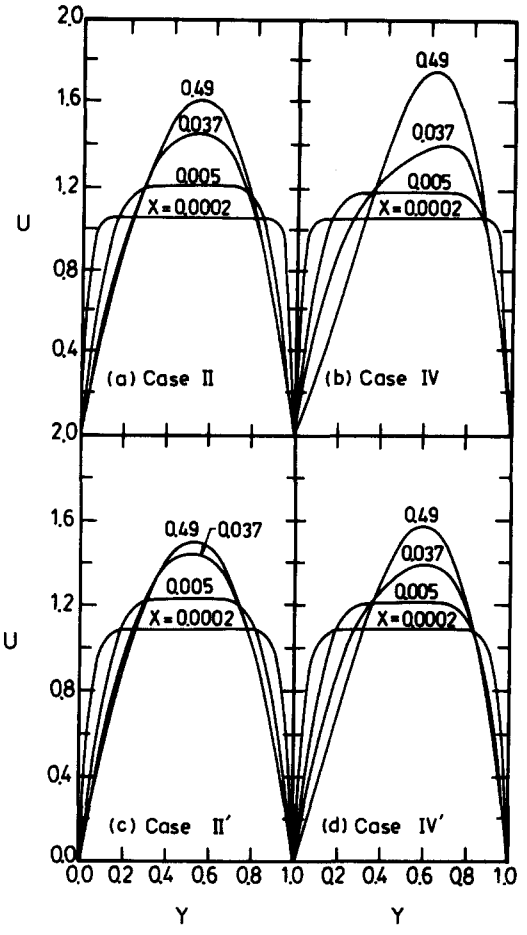

Figure 1 Developments of dimensionless axial velocity profiles: (a) $T_0=20$°C, $T_1=50$°C, $T_2=30$°C, Re=2000, $\phi=50$%; (b) Re=500. The conditions of case II' and IV' are the same as those of cases II and IV, except no liquid films on the channel's surfaces

it was found that the distributions of the temperature and mass fraction are slightly different for the cases with or without concentration buoyancy. Despite the effects of mass diffusion buoyancy on the θ and W are small, the mass diffusion effects could cause an enhancement of heat transfer on the channel walls.

It is of interest to examine the effects of buoyancy forces of thermal and mass diffusion on the distributions of pressure defect in the flow. This is indicated in Figure 4. It is clear from this plot that for low T_1 and high Re (cases I and II) the motion pressure is always negative and decreases with X, similar to that in pure forced convection. While for high T_1 and low Re in cases III and IV (high Gr_T/Re and Gr_M/Re), the motion pressure first decreases and stays negative, and then increases and becomes positive as the fluid moves downstream—an adverse pressure gradient. This confirms the results of other

Table 2 Values of major parameters for various cases

Case	T_1	T_2	Re	Gr_T	Gr_M	Pr	Sc	S_1	S_2
I	30	30	2000	4652.6	1598.1	0.705	0.594	5.38	5.38
II	50	30	2000	12973.3	5667.6	0.703	6.52		6.67
III	70	30	2000	20165.0	15059.2	0.702	0.589	10.97	11.49
IV	50	30	500	12973.3	5567.6	0.703	0.592	6.52	6.67
V	70	30	500	20165.0	15059.2	0.702	0.589	10.97	11.49

$T_0=20$°C, $\phi=50$%, and $b=1.5$ cm.

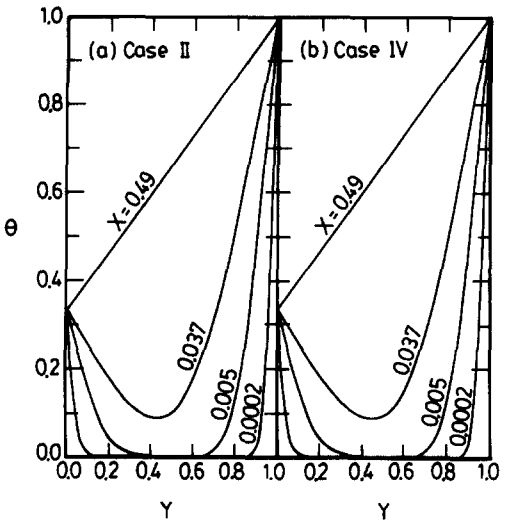

Figure 2 Developments of dimensionless temperature profiles: (a) $T_0=20°C$, $T_1=50°C$, $T_2=30°C$, Re=2000, $\phi=50\%$; (b) Re=500

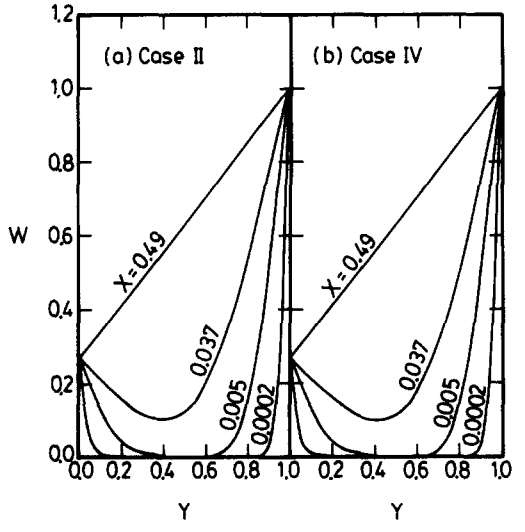

Figure 3 Developments of dimensionless mass-fraction profiles: (a) $T_0=20°C$, $T_1=50°C$, $T_2=30°C$, Re=2000, $\phi=50\%$; (b) Re=500

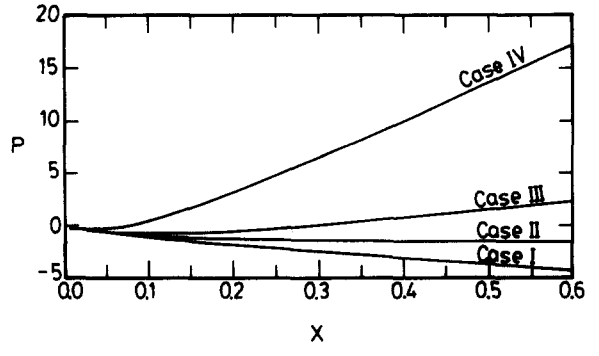

Figure 4 Dimensionless motion pressure distributions along the channel: case I, $T_0=20°C$, $T_1=T_2=30°C$, Re=2000, $\phi=50\%$; case II, $T_1=50°C$; case III, $T_1=70°C$; case IV, $T_1=50°C$, Re=500

studies.[11,17–19] The above features can be made plausible by noting that under the conditions of low T_1 and high Re (low Gr_T/Re and Gr_M/Re), the buoyancy effects are weak. Therefore, the mixed convection in the channel is closer to forced convection. While for high T_1 and low Re the buoyancy effects are significant. Thus, the frictional force in the flow is overwhelmed by the positive buoyancy forces, which, in turn, causes an adverse pressure gradient.

To demonstrate the relative contributions of heat transfer through sensible and latent heat exchanges in the flow, three kinds of Nusselt numbers along the right and left wetted walls are presented in Figures 5 and 6, respectively. An overall inspection on Figures 5(a) and 5(b) shows that the heat transfer due to the transport of latent heat is much more effective than that due to the transport of the sensible heat on the right wall. Furthermore, a larger Nu_{l1} is found for the system with a higher T_1 (by comparing cases II and III). This is brought about by the larger latent heat transfer in association with the larger water vapor evaporation for a higher T_1. Focusing on Figure 5(a), we note that Nu_{s1} is slightly larger for the system with a lower T_1 (by comparing II and III). This is a direct consequence of the finding by Carter and Gill[20]—larger water vapor evaporation associated with higher T_1 causes the temperature profiles to become flattened which then results in less sensible heat transfer. In Figure 5(c), Nu_{x1}, the sum of Nu_{s1} and Nu_{l1}, is presented.

The influence of Re on the heat transfer is also of importance. Comparison of cases II and IV in Figures 5(a) and 5(b) indicates that both the sensible and latent heat transfer are more effective

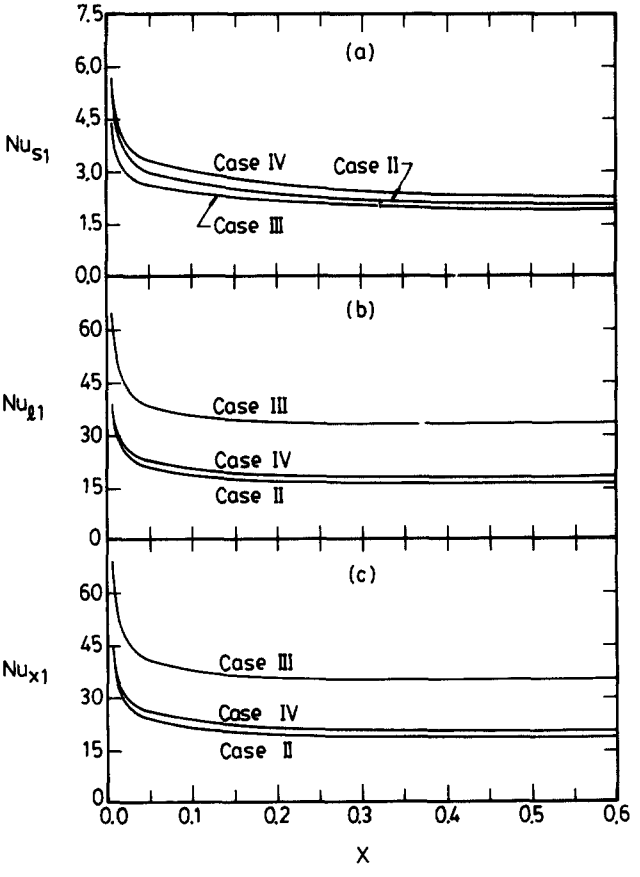

Figure 5 Local Nusselt numbers for (a) sensible heat; (b) latent heat; (c) overall along the right wetted wall: case II, $T_0=20°C$, $T_1=50°C$, $T_2=30°C$, Re=2000, $\phi=50\%$; case III, $T_1=70°C$; case IV, $T_1=50°C$, Re=500

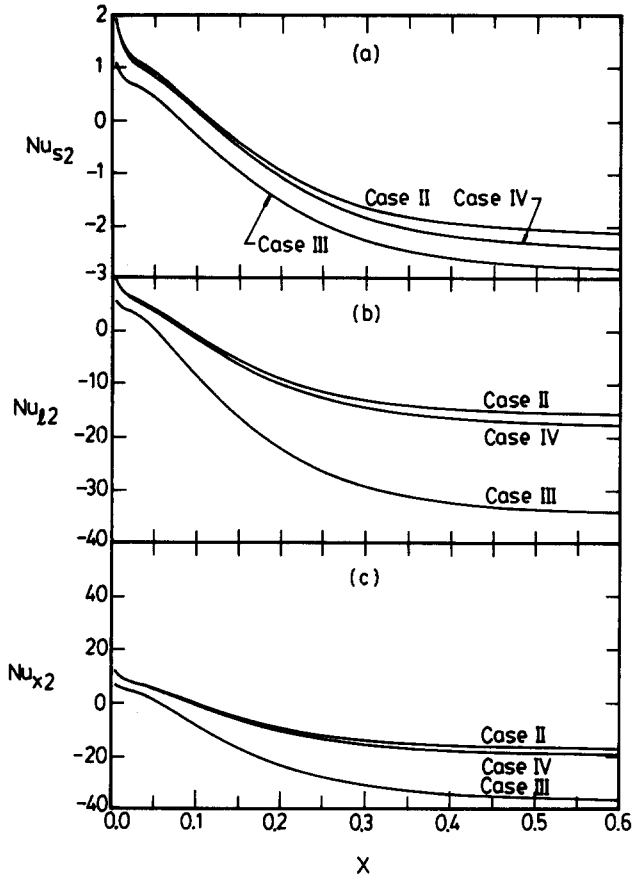

Figure 6 Local Nusselt numbers for (a) sensible heat; (b) latent heat; (c) overall along the left wetted wall: case II, $T_0=20°C$, $T_1=50°C$, $T_2=30°C$, Re=2000, $\phi=50\%$; case III, $T_1=70°C$; case IV, $T_1=50°C$, Re=500

for the flow with a lower Re owing to the larger buoyancy effects (higher Gr_T/Re and Gr_M/Re).

Shown in Figure 6 are the distributions of the local Nusselt numbers along the left wetted wall whose temperature is fixed at $T_2=30°C$. Careful scrutiny on Figures 6(a) and 6(b) reveals that in the initial portion of the channel, Nu_{s2} and Nu_{l2} are both positive. But as the moist air moves further downstream, Nu_{s2} and Nu_{l2} change sign and become negative. Moreover, the locations after which Nu_{s2} and Nu_{l2} become negative are closer to the channel entrance for the system with a higher T_1. The change of sign in Nu_{l2} is undoubtedly connected with the direction of mass diffusion on the left wetted wall. Near the channel entrance, the liquid films evaporate and generate vapor into the air stream from both wetted walls because of the low concentration of water vapor in the air stream in this region. Therefore the direction of latent heat transfer is from the wall to the air stream on the left wetted wall. But as the moist air goes downstream, due to the significant evaporation of the liquid film from the right wetted wall which is at a higher temperature, the mass-fraction of water in the flow could be over w_2 after certain axial location, as just discussed (Figure 3). As a result, the condensation of water vapor would occur on the left wetted wall, which, in turn, results in a negative Nu_{l2} along the wetted wall.

The variations of local Sherwood number along the wetted walls, illustrated in Figure 7, are similar in trend to those of the sensible Nusselt number. Since the temperature of the right wetted wall is maintained at a higher level than that of the left wetted wall (except for case I, the symmetric heating case), the water vapor always moves into the air stream from the right wetted wall, and hence Sh_1 is all positive. But on the left wetted wall Sh_2 is negative in the downstream region. This again indicates that in the downstream region, condensation of water vapor occurs on the left wetted wall.

To illustrate the effectiveness of latent heat transfer through mass diffusion, the heat transfer rate from the wetted walls is contrasted with the result for the situation in which the channel walls are not wetted. The results for Q_1/Q_1'' are given in Figure 8, here Q_1'' represents the actual heat transfer rate from the right wetted wall under the same condition for each case except no liquid water films on the channel's surfaces. It is clearly seen that the tremendous capacity of energy transport through mass diffusion is demonstrated by noting that Q_1/Q_1'' can be as large as 15 for case V ($T_1=70°C$, Re=500).

The net amount of the water vapor from liquid film vaporization added to the air stream is important in improving

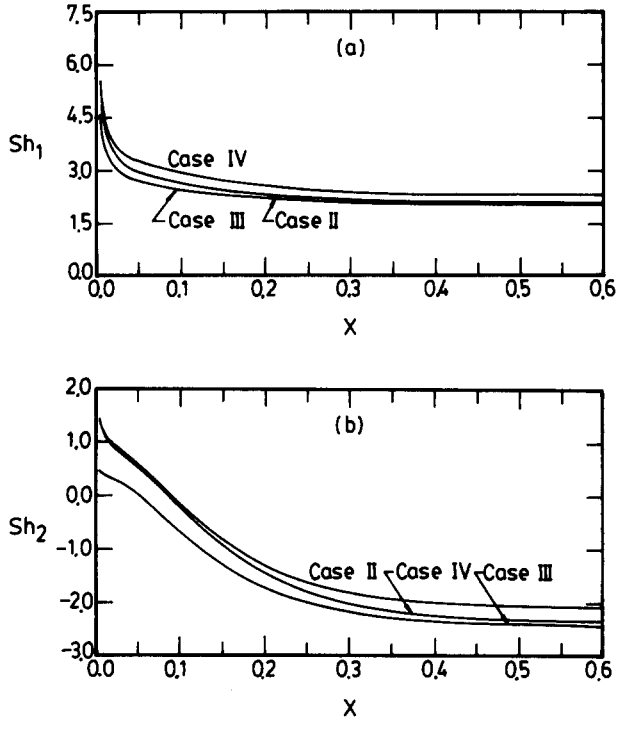

Figure 7 Local Sherwood number along the wetted walls: case II, $T_0=20°C$, $T_1=50°C$, $T_2=30°C$, Re=2000, $\phi=50\%$; case III, $T_1=70°C$; case IV, $T_1=50°C$, Re=500

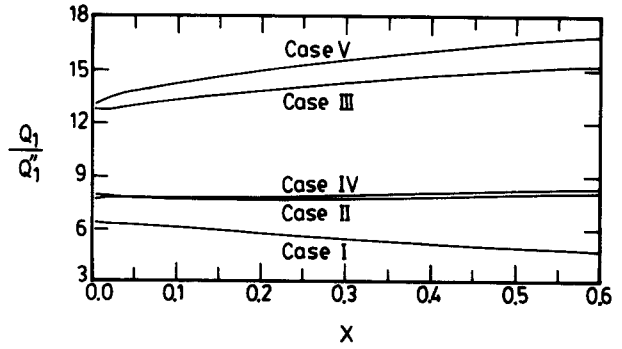

Figure 8 Effects of system temperatures and the Reynolds number in the flow on the total heat transfer rate: case I, $T_0=20°C$, $T_1=T_2=30°C$, Re=2000, $\phi=50\%$; case II, $T_1=50°C$; case III, $T_1=70°C$; case IV, $T_1=50°C$, Re=500; case V, $T_1=70°C$, Re=500

our understanding on the heat and mass transfer rate. To this end, a nondimensional net mass flow rate resulting from the evaporation or condensation on the wetted walls is introduced

$$M_{ri} = \frac{\text{mass flow rate added to the air stream from wetted wall } i}{\text{inlet mass flow rate}}$$

$$= \begin{cases} -\int_0^x \rho v_1 \dfrac{dx}{\rho u_0 b} & 17a) \\ \int_0^x \rho v_2 \dfrac{dx}{\rho u_0 b} & (17b) \end{cases}$$

in dimensionless variables

$$M_{r1} = -\int_0^X V_1 \, dX \qquad (18a)$$

$$M_{r2} = \int_0^X V_2 \, dX \qquad (18b)$$

The effects of system temperatures and Re on the distributions of M_{ri} along the wetted walls are presented in Figure 9. The results in Figure 9(a) apparently indicate that along the right wetted wall, a large vapor vaporization is experienced for a system with a higher T_1. The mass addition to the flow is mainly dependent on channel wall temperatures with the effect of Re being insignificant.

As for the net vapor mass flow rate entering the air stream from the left wetted wall (Figure 9(b)), except for case I, M_{r2} increases with X up to certain axial location and then decreases with X due to the occurrence of the condensation of water vapor on the left wetted wall.

In the present study, the boundary-layer approximations were adopted to simplify the analysis. Therefore, it is important to check whether the transverse velocity is small compared

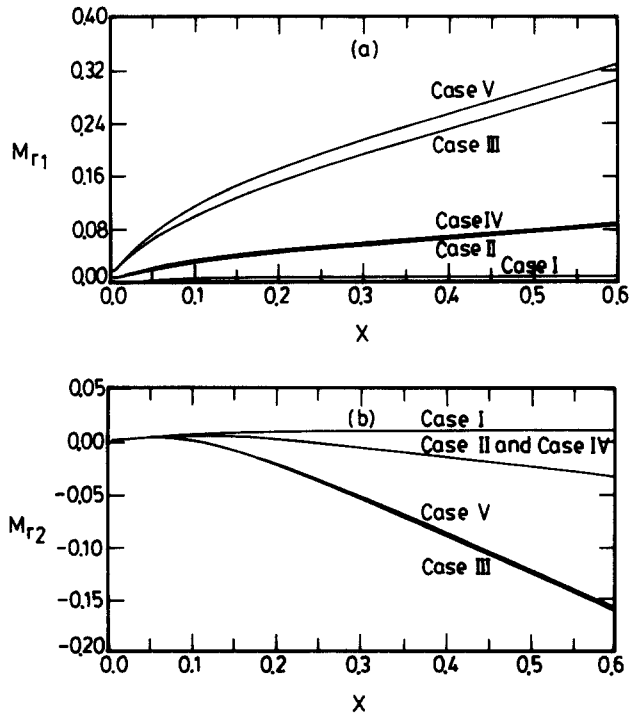

Figure 9 Effects of system temperatures and the Reynolds number in the flow on the net mass flow rates entering into air stream from both wetted walls: case I, $T_0 = 20°C$, $T_1 = T_2 = 30°C$, Re = 2000, $\phi = 50\%$; case II, $T_1 = 50°C$; case III, $T_1 = 70°C$; case IV, $T_1 = 50°C$, Re = 500; case V, $T_1 = 70°C$, Re = 500

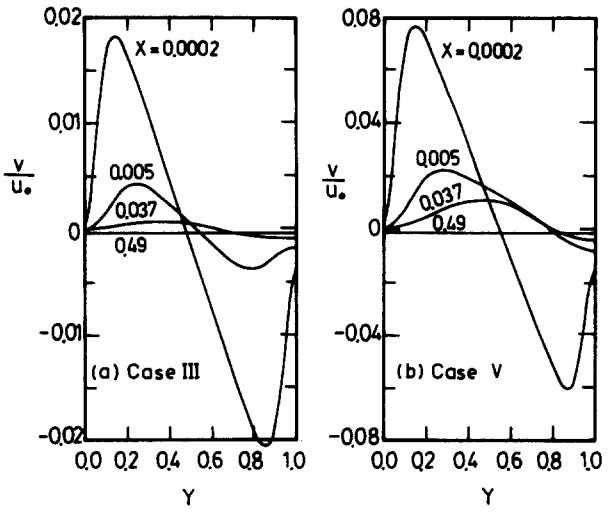

Figure 10 Developments of dimensionless velocity ratio V_r

with the axial velocity. To this end, a nondimensional velocity ratio V_r is introduced

$$V_r = v/u_0 = 2V/\mathrm{Re} \qquad (19)$$

It is clearly seen in Figure 10 that the velocity ratio V_r is rather small, except near the inlet (at $X = 0.0002$). Therefore, in the present study the boundary-layer approximations are valid.

Conclusions

Laminar mixed convection flows in a vertical channel under the simultaneous influences of the combined buoyancy effects of thermal and mass diffusion has been studied, particularly for the air–water system. The effects of the wetted wall temperatures and the Reynolds number of the flow on the transfer of momentum, heat and mass tranfer in the flow were examined in great detail. What follows is brief summary of the major results:

(1) Heat transfer in the flow is dominated by the transport of latent heat in connection with the evaporation or condensation of the water vapor along the wetted walls.
(2) Because of the larger amount of water vapor evaporated into the air stream for the system with a higher T_1, the axial location where the condensation of water vapor begins to occur on the left wetted wall is closer to the channel entrance when T_1 is higher.
(3) A higher T_1 results in a larger V_1 in the entry region, which, in turn, causes the temperature profiles to become flattened near the right wetted wall and thus give a lower value for Nu_{s1}.
(4) The presence of the mass diffusion effect causes pronounced heat transfer enhancement.

Acknowledgment

The financial support of this work by National Science Council of Taiwan, Republic of China is greatly appreciated.

References

1 Chen, T. S. and Yuh, C. F. Combined heat and mass transfer in natural convection on inclined surfaces. *Numer. Heat Transfer*, 1979, **2**, 233–250

2 Chen, T. S. and Yuh, C. F. Combined heat and mass transfer in natural convection along a vertical cylinder. *Int. J. Heat Mass Transfer*, 1980, **23**, 451–461

3 Gill, W. N., Casal, E. D., and Zeh, D. W. Binary diffusion and heat transfer in laminar free convection boundary layers on a vertical plate. *Int. J. Heat Mass Transfer*, 1965, **8**, 1135–1151

4 Hason, M. and Mujumdar, A. S. Coupled heat and mass transfer in natural convection under flux condition along a vertical cone. *Int. Commun. Heat Mass Transfer*, 1984, **11**, 157–172

5 Chang, C. J. and Lin, T. F. and Yan, W. M. Natural convection flows in a vertical open tube resulting from combined buoyancy effects of thermal and mass diffusion. *Int. J. Heat Mass Transfer*, 1986, **29**, 1543–1552

6 Lee, T. S., Parikh, R. G., Acrivos, A., and Bershader, D. Natural convection in a vertical channel with opposing buoyancy forces. *Int. J. Heat Mass Transfer*, 1982, **25**, 499–511

7 Chow, L. C. and Chung, J. N. Evaporation of water into a laminar stream of air and superheated steam. *Int. J. Heat Mass Transfer*, 1983, **26**, 373–380

8 Wu, C. H., Davis, D. C., Chung, J. N., and Chow, L. C. Simulation of wedge-shaped product dehydration using mixtures of superheated steam and air in laminar flow. *Numer. Heat Transfer*, 1987, **11**, 109–123

9 Santarelli, F. and Foraboschi, F. P. Heat transfer in mixed laminar convection in a reacting fluid. *Chem. Eng. J.*, 1973, **6**, 59–68

10 Yeh, H. M., Tsai, S. W., and Yang, C. C. Heat and mass transfer in mixed convection over a horizontal plane. *Numer. Heat Transfer*, 1987, **12**, 229–242

11 Lin, T. F., Chang, C. J., and Yan, W. M. Analysis of combined buoyancy effects of thermal and mass diffusion on laminar forced convection heat transfer in a vertical tube. *J. Heat Transfer*, 1988, **110**, 337–344

12 Hubbard, G. L., Denny, V. E., and Mills, A. E. Droplet evaporation: effects of transients and variable properties. *Int. J. Heat Mass Transfer*, 1975, **18**, 1003–1008

13 Fujii, T., Kato, Y., and Mihara, K. Expressions of transport and thermodynamic properties of air, steam and water. Sei. San Ka Gaku Ken Kyu Jo, Report No. 66, Kyu Shu Dai Gaku, Kyu Shu, Japan, 1977

14 Eckert, E. R. G. and Drake, R. M., Jr. *Analysis of Heat and Mass Transfer*. Chapters 20, 22, McGraw-Hill, New York, 1972

15 Manganaro, J. L. and Hanna, O. T. Simultaneous energy and mass transfer in the laminar boundary layer with large mass transfer rates toward the surface. *A.I.Ch.E.J.*, 1970, **16**, 204–211

16 Patankar, S. V. *Numerical Heat Transfer and Fluid Flow*. Chapter 4, Hemisphere and McGraw-Hill, New York, 1980

17 Aung, W. and Worku, G. Developing flow and flow reversal in a vertical channel with asymmetric wall temperatures. *J. Heat Transfer*, 1986, **108**, 299–304

18 Aung, W. and Worku, G. Theory of fully developed, combined convection including flow reversal. *J. Heat Transfer*, 1986, **108**, 485–488

19 El-Shaarawi, M. A. I. and Sarhan, A. Free convection effect on the developing laminar flow in vertical concentric annuli. *J. Heat Transfer*, 1980, **102**, 617–622

20 Carter, L. F. and Gill, W. N. Asymptotic solution for combined free and forced convection in vertical and horizontal conduits with uniform suction and blowing. *A.I.Ch.E.J.*, 1964, **10**, 330–339